



**Diseño de estrategias de control PID y MPC para un campo de colectores solares distribuidos virtual.**

Chimbana Masabanda, Lenin Israel y Muyón Rivera, Kevin Paúl

Departamento de Eléctrica y Electrónica

Carrera de Ingeniería en Electrónica e Instrumentación

Artículo académico, previo a la obtención del título de Ingeniera en Electrónica e Instrumentación

Dr. Llanos Proaño, Jacqueline del Rosario

8 de diciembre del 2022

Latacunga

# PID and Model Predictive Control (MPC) Strategies Design for a Virtual Distributed Solar Collector Field.

Kevin Muyón<sup>1</sup>[0000-0001-9792-0863], Lenin Chimbana<sup>1</sup>[0000-0003-3589-5329], Jacqueline Llanos<sup>1</sup>[0000-0002-6708-3897] and Diego Ortiz-Villalba<sup>1</sup>[0000-0001-8584-8921]

<sup>1</sup> Universidad de las Fuerzas Armadas ESPE, Sangolqui, Ecuador  
kpmuyon@espe.edu.ec, lichimbana@espe.edu.ec, jdllanos1@espe.edu.ec  
, ddortiz5@espe.edu.ec

**Abstract.** Distributed solar collector fields are an interesting case in the area of control since apart from presenting several disturbances, their main source of energy is solar irradiation that cannot be manipulated, depends on daily and seasonal variations causing the solar resource is not always available. This makes it necessary to research control techniques that can optimize the use of the existing solar resource. Therefore, in this research, a model predictive control strategy MPC is designed for a virtual distributed solar collector field where the control objective is to maintain the output temperature of a fluid at the desired value. In addition, a PID control strategy with a Feedforward block is also implemented that it's used to compare the results obtained with the MPC to determine which controller has better performance, which one allows a longer operation time, optimizing the use of the available solar irradiation and which one responds better to disturbances. All this is through an immersive virtual environment where the user can interact with all the instrumentation of the virtual distributed solar collector field and can visualize the evolution of the variables and modify the state of the virtual plant by manipulating the disturbances as well as the parameters of the PID and MPC controllers designed. Finally, the results show a better performance of the plant when implementing the MPC control strategy and the advantages of implementing a virtual environment interactive with the user.

**Keywords:** Model Predictive Control, Solar Collector Field, Virtual Industrial Process.

## 1 Introduction

The electricity demand has grown over the years due to social and economic development and the improvement of people's living conditions. In this context, the predominant energy source since 1850 has been fossil fuels which has led to a rapid increase in carbon dioxide emissions [1]. It is for this reason and due to the 1973 oil crisis that renewable energies received a strong impulse and new ways of obtaining energy through solar irradiation began to be developed, one of these technologies is the distributed solar collector fields such as the ACUREX field located in Almeria, Spain [2].

Distributed solar collector field plants have non-linear dynamics, are affected by various disturbances such as ambient temperature, inlet temperature and depend on solar irradiance which cannot be manipulated and is not always available making it necessary to take full advantage of the solar resource [3].

It is because of all these characteristics that the distributed solar collector field is a very interesting system in the area of implementing control techniques that can cope with changes in solar irradiation, existing disturbances while optimizing the plant operation time, maximizing the solar resource and fulfilling the safety conditions of the plant.

Since having real industrial processes for experimental tests represents a high investment of money, it is necessary to look for methodologies such as the virtualization of industrial processes where control techniques can be implemented at the same time that the real behavior of the process can be simulated, such as those that have been developed in [4] where a virtual laboratory of a combined cycle thermal power plant is implemented, virtual laboratory of multivariable level and temperature processes in [5], design and implementation of a predictive control model for a pressure control plant in [6], model predictive control strategy for a combined-cycle power-plant boiler in [7], advanced control algorithms for a horizontal three-phase separator in a hardware in the loop simulation environment in [8], which allow us to implement traditional controllers and advanced controllers in order to implement the best controller for the process. However, virtual laboratories have not been developed in the renewable energy sector that base their operation on solar irradiation such as a distributed solar collector field.

This is why, in this research, a virtual environment of a distributed solar collector field based on the ACUREX field is designed, in which a model predictive control MPC strategy can be tested with a PID control strategy to validate the MPC controller.

The main contributions of this paper are *i)* An immersive environment that allows the user to interact with the virtual distributed solar collector field, *ii)* The design of a PID control strategy for the implementation in the virtual distributed solar collector field *iii)* The design of model predictive control MPC for the implementation in the virtual distributed solar collector field.

For the development of this research the next methodology is followed where section 2 shows the description of the plant and the mathematical model, then section 3 shows the steps to implement the virtualization, and finally, section 4 shows the design of the control algorithms.

## **2 Description and Mathematical Model of the Virtual Distributed Solar Collector Field**

This section describes the operation of the virtual distributed solar collector field and the mathematical model implemented for the virtual plant.

## 2.1 Description of the Virtual Distributed Solar Collector Field

The distributed solar collector field uses solar irradiation as an energy source to heat a fluid that circulates through the solar collectors, this hot fluid can be used at a later stage for electric power generation or water desalination [9], the fluid outlet temperature also depends of other factors such as the fluid inlet temperature and the ambient temperature.

As can be seen (see Fig. 1), the virtual distributed solar collector field implemented in this research has two storage tanks that store the hot fluid and the cold fluid respectively, it has solar tracking to ensure that solar radiation is reflected on the reflecting mirrors of the solar collectors and is received by the tube that transports the fluid, thus heating the cold fluid that enters the solar collector field to a maximum temperature of  $300[^\circ\text{C}]$ , the temperature control is performed by manipulating the flow rate of the fluid that circulates through the solar collectors. The fluid used is Santotherm 55 oil, which is a thermal oil that allows working with temperatures higher than  $300[^\circ\text{C}]$ .

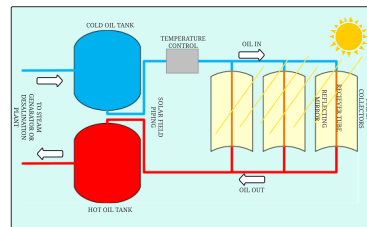


**Fig. 1.** Elements of the virtual distributed solar collector field.

To better understand the operation of the virtual distributed solar collector field implemented in this paper, the piping and instrumentation diagram P&ID (see Fig. 2) shows the instrumentation and components of the entire plant.

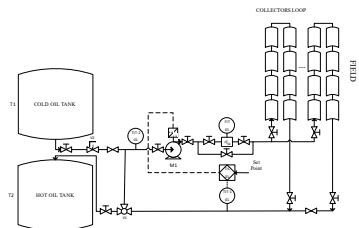


**Fig. 2.** P&ID diagram of the virtual distributed solar collector field.

At the beginning and end of the day when solar irradiation is below  $400[W/m^2]$  the plant is not operating as this is the minimum temperature for start-up, so the plant is in sleep mode, once the plant is in operation it can be in 2 different modes which are recirculation mode and tank mode [10].

The objective of control loop 01 is to maintain the oil outlet temperature at the end of the collector's loop at the desired level, the control loop 01 consists of a temperature

indicator transmitter (TIT-1) that sends the temperature value of the outlet oil to the temperature indicator controller (TIC), this is responsible for sending the control signal to the hydraulic pump (M1), the hydraulic pump (M1) is used to modify the amount of oil flow that circulates through the solar collector field by decreasing the oil flow to heat the fluid or increasing the oil flow to cool the fluid, the oil flow varies from 0.002 to 0.012 [ $m^3/s$ ] where the lower limit is used so that the oil outlet temperature does not exceed 305 [ $^{\circ}C$ ] because if it exceeds 305 [ $^{\circ}C$ ] the oil could decompose [11].

Additionally, loop 01 consists of a second temperature indicator transmitter (TIT-2) and a flow indicator transmitter (FIT) which are used for the operator to visualize the oil inlet temperature and oil flow respectively. The plant is also equipped with a cold oil tank (T1) which is used to store the oil that will be heated in the solar collector field, once the oil is heated it is stored in the hot oil tank (T2), there is also a 3-way valve (V1) that is responsible for recirculating the oil flow inside the collector loop which is initially at a very low temperature and finally, there is a valve (V2) that allows the circulation of the fluid inside the cold oil tank to the collector field.

## 2.2 Mathematical Model of the Virtual Distributed Solar Collector Field

The model used for this paper is the distributed parameter model displayed in [9] which corresponds to the ACUREX field that is part of one of the installations of the Almeria Solar Platform located in the Tabernas desert (Almeria, Spain) and has been used as a test laboratory for different experiments and control structures, in addition to detailing each loop of parabolic collectors that constitute the plant.

The distributed parameter model adequately shows the dynamics of the distributed solar collector field since it simulates well the temperature distribution by applying the conservation of energy in a length  $dl$  over a time interval  $dt$  along the collector loop, modeling separately the oil fluid and the metal tube as shown in equation 1 and equation 2.

$$A_m \rho_m C_m \frac{dT_m(t,l)}{dt} = \eta GI(t) - D_m \pi H_l (T_m(t,l) - T_{amb}(t,l)) - D_f \pi H_t (T_m(t,l) - T_f(t,l)) \quad (1)$$

$$A_f \rho_f C_f \frac{dT_f(t,l)}{dt} + \rho_f c_f q(t) \frac{dT_f(t,l)}{dl} = D_f \pi H_t (T_m(t,l) - T_f(t,l)) \quad (2)$$

In equations 1 and 2 the subindices  $m$  refer to the metal tube while  $f$  refer to the oil fluid. Where  $A$  is the transversal section [ $m^2$ ],  $\rho$  the density [ $kg/m^3$ ],  $C$  the thermal capacity [ $J/kg^{\circ}C$ ],  $T$  the temperature [ $^{\circ}C$ ],  $\eta$  the collector efficiency,  $G$  the aperture of the collector [ $m$ ],  $I$  the solar irradiation [ $W/m^2$ ],  $T_{amb}$  the ambient temperature [ $^{\circ}C$ ],  $D$  the external diameter [ $m$ ],  $H_l$  the global coefficient of thermal losses [ $W/m^2^{\circ}C$ ],  $H_t$  the heat transfer coefficient metal-oil [ $W/m^2^{\circ}C$ ],  $q$  the oil flow [ $m^3/s$ ],  $t$  the time [ $s$ ],  $l$  the length [ $m$ ], a more detailed description of the parameters used in the model can be found in [12].

As can be seen (see Fig. 3), the inputs for the virtual plant are the oil inlet temperature  $T_{in}$ , the ambient temperature  $T_{amb}$ , the irradiance  $I$ , the oil flow  $q$ , and the output parameter is the oil outlet temperature  $T_f$  at the end of the collector loop.

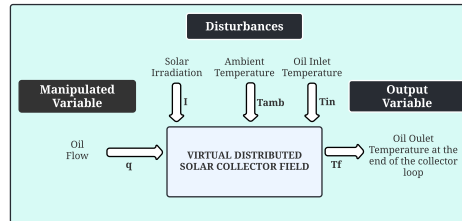


Fig. 3. Variables of the virtual distributed solar collector field.

### 3 Virtualization Methodology

Nowadays, technological progress has allowed the implementation of virtual laboratories in the area of medicine, education, and particularly in industry, which makes it easier to understand and become familiar with the industry through virtual environments that emulate a real process, as shown in [13].

This is why a virtualization methodology (see Fig. 4) is applied to design a virtual environment that resembles a real distributed solar collector field, where it is possible to visualize all the instrumentation of the plant, the evolution of the variables, and manipulate the behavior of the plant.

The environment is designed in the UNITY 3D graphic engine. The methodology consists of 5 layers: *i*) Layer 1. In this layer we start with the virtualization of the solar collector field through the 3D design of the elements that conform to the P&ID diagram through a CAD software, *ii*) Layer 2. Layer that allows the export of the graphic models developed in layer 1 to a format compatible with the Unity 3D graphic engine, as well as modifying characteristics of the 3D models such as reference axes, rotation axes, colors, textures, etc. *iii*) Layer 3. This layer allows to design of the virtual environment in Unity using the 3D models designed in the previous layers, adding animations and response curves, making the environment immersive and intuitive. *iv*) Layer 4. In this research the shared memory method is implemented to allow bilateral communication, this is through the use of a dynamic link library DLL that generates a shared memory in the RAM for the exchange of the process variables data between the 3D environment in Unity and the mathematical software Matlab, such as solar irradiance, ambient temperature, oil inlet temperature, set point, oil outlet temperature, oil flow. The method of shared memories is used because it is an easy technique to apply, with short delays and low computational cost as shown in [14] *v*) Layer 5. In this layer are the mathematical model and the designed controllers of the virtual plant that are implemented in the Matlab software.

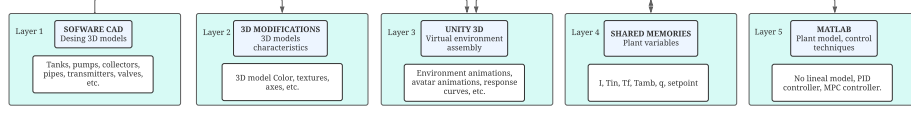


**Fig. 4.** Virtualization methodology of the virtual distributed solar collector field.

## 4 Design of Control Algorithms

The distributed solar collector field is an interesting case study in the area of control since it is affected by several disturbances such as ambient temperature, inlet oil temperature and its main source of energy solar irradiation also acts as a disturbance since it cannot be manipulated and suffers from daily variations and is not always available. All the aspects mentioned make it necessary to find an adequate control strategy that can cope with the changes in solar irradiation as well as increase the plant operation time by optimizing the use of the available solar resource, all this while complying with the plant safety conditions such as the maximum temperature of the oil.

For this reason, in this section, it is designed an MPC control and additionally a PID control with a feedforward block that will be used to analyze the performance of the MPC, where the control objective is to maintain the oil outlet temperature at the desired level.

### 4.1 PID Control Strategy Design

Although the output of this process is affected by several disturbances, the solar irradiance, and the oil inlet temperature are the ones that most affect the process, causing the control action, oil flow, by itself to be insufficient to bring the response of the plant to a steady state since the oil outlet temperature would have a similar trend to the solar irradiance profile and the oil inlet temperature, therefore, the system response is more affected by the disturbances than by the control action, making the system identification process and the PID control design more difficult.

Since these disturbances are measurable, a Feedforward block is implemented, which takes this information and attenuates the changes produced by the disturbances, making the necessary corrections to the control action. The feedforward block used is shown in equation 3. Where  $u$  represents the output of the PID control, this equation has been developed experimentally in [15] and widely implemented in experiments carried out in the ACUREX field.

$$q = \frac{0.7869I - 0.485(u - 151.5) - 80.7}{u - T_{in}} \quad (3)$$

The PID control is implemented in series with the Feedforward block (see Fig. 5) which acts as part of the plant mitigating the effect of disturbances to facilitate the control PID tuning.

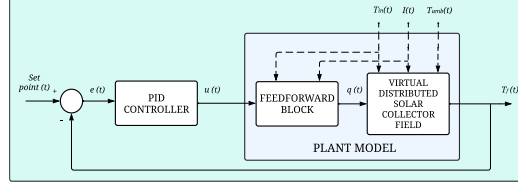


**Fig. 5.** PID control strategy with a feedforward block implemented in the virtual distributed solar collector field.

The control strategy is defined by equation 4. Where  $u$  is the control action,  $K_p$  is the proportional gain,  $T_i$  is the integral time gain, and  $T_d$  is the derivative time gain. To obtain the control gains, the Lambda tuning method was used [16].

$$u(t) = K_p \left( e(t) + \frac{1}{T_i} \int_0^t e(t) dt + \frac{1}{T_d} \frac{d}{dt} e(t) \right) \quad (4)$$

#### 4.2 Model Predictive Control MPC Strategy Design

A model predictive control MPC consists of a prediction model, cost function, and constraints, the particularity of this controller is that it uses a prediction model that allows to know the future behavior of the controlled variable using a prediction horizon  $N_w$  and a control horizon  $N_c$  [17]. The MPC includes a cost function which has as its first objective to minimize the oil outlet temperature errors and has as its second objective to smooth the abrupt variations of the control action as detailed in equation 5.

$$J(k) = \sum_{i=N_w}^{N_p} \delta(k) \left[ \hat{T}_f(k+i|k) - T_{fd}(k+i|k) \right]^2 + \sum_{i=0}^{N_c-1} \lambda(k) [\Delta u(k+i-1)]^2 \quad (5)$$

Where the first term  $\left[ \hat{T}_f(k+i|k) - T_{fd}(k+i|k) \right]^2$  is the squared error between the desired value and the predicted value of the oil outlet temperature,  $\delta(k)$  is the weight for the first control objective, the objective function also includes the squared variation of the control action  $[\Delta u(k+i-1)]^2$ , where  $\lambda(k)$  represents the weight of the second control objective, additionally  $N_p$  represents the total number of samples of the prediction horizon.

The optimization problem considers oil flow operation constraints as in equation 6.

$$q_{\min} \leq q \leq q_{\max} \quad (6)$$

Where the values of the constraints are  $q_{\min} = 0.0002 [m^3/s]$  and  $q_{\max} = 0.0012 [m^3/s]$ , these limits help to keep the temperature below  $305 [^\circ C]$ . Finally, (see Fig. 6) shows the MPC strategy implemented in the virtual distributed solar collector field.

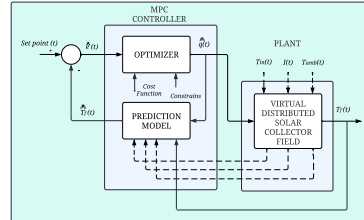


**Fig. 6.** Model predictive control MPC strategy implemented in the virtual distributed solar collector field.

## 5 Results

This section describes the results obtained in the development of the virtual environment, as well as in the design of the PID and MPC control strategies, analyzing the virtual environment designed, the interactivity and immersivity, also the response of each controller, which one reacts better to disturbances, which one allows longer operation time and which one satisfies the security conditions of the virtual distributed solar collector field.

### 5.1 Analysis of the Virtual Distributed Solar Collector Field Implemented

Once the virtualization strategy of section 3 has been implemented, the results of the virtualized solar collector field environment are shown (see Fig. 7) which resembles a real distributed solar collector field plant.

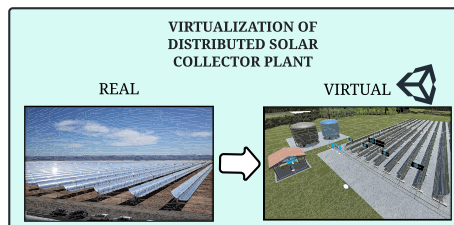


**Fig. 7.** Virtual distributed solar collector field compared to a real solar collector field.

For the visualization and control of the virtual distributed solar collector field there is a control room (see Fig. 8), where there are several screens that allow to visualize the status of the virtual plant showing if the plant is in sleep mode, recirculation mode or tank mode as well as alerts on the outlet temperature and solar irradiation, it also shows the evolution of the variables of interest such as: solar irradiation, ambient temperature, oil inlet temperature, oil outlet temperature, oil flow, as well as sliders and interactive buttons where the user can manipulate the set point value, the value of the oil inlet temperature, add the presence of clouds in the solar irradiance and be able to select

between PID control and MPC as well as being able to modify the tuning constants of both controllers.

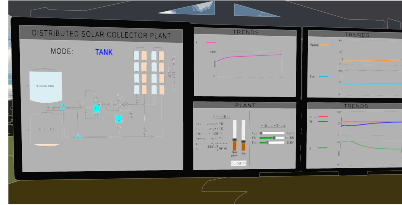


**Fig. 8.** Control room of the virtual distributed solar collector field.

The virtual plant also has animations (see Fig. 9a) such as filling the storage tanks, solar tracking of the solar collectors, changing solar irradiance, and avatar control, allowing the user to understand the operation of a field of distributed solar collectors while moving through the virtual environment.

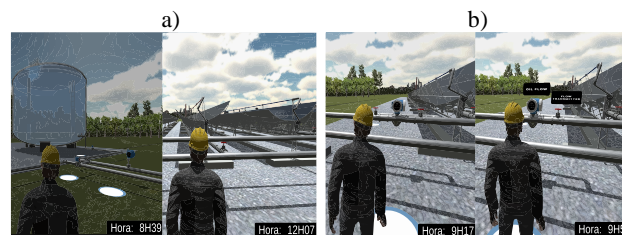


**Fig. 9.** a) Animations inside the virtual distributed solar collector field, b) Interactivity between the user and the components of the virtual distributed solar collector field.

Finally, to ensure interactivity between the user and the solar collector field, each component that compounds the virtual plant has an interactive element that is activated when the user approaches it, displaying important information for the operator (see Fig. 9b).

The environment was tested with different students where they were able to design the PID and MPC controllers by manipulating the tuning constants, visualize through the graphs the evolution of the variables that affect the virtual plant, and interact with the instruments of the virtual plant by identifying the type of instrument and its function.

## 5.2 Analysis of the Control Strategies Implemented in the Virtual Distributed Solar Collector Field

To validate the design of the MPC implemented in the virtual distributed solar collector field, the results obtained are compared with the PID control designed for this purpose, 3 scenarios are analyzed *i*) Day with high solar irradiation, *ii*) Day with medium solar irradiation, *iii*) Day with medium solar irradiation, but with the presence of clouds and

variation in the oil inlet temperature. The response of the virtual plant is shown from 8:00 to 18:30.

The solar irradiation and ambient temperature profiles for these scenarios correspond to the Almeria solar platform in December for scenario *i*) and in June for scenario *ii*). These profiles are obtained through the European Commission Photovoltaic Geographical Information System [18], for scenario *iii*) the data of scenario *ii*) is taken by adding the presence of clouds in the solar irradiation and varying the value of the oil inlet temperature.

The following control parameters are used for the PID control,  $K_p=0.03$ ,  $T_i=70.55$ ,  $T_d=2.86$ . For the MPC the design parameters are, the value of the weight for the oil outlet temperature error is  $\delta=10000$ , the weight for the control action is  $\lambda=1$ , for the prediction horizon we have  $N_w=10$ , and for the control horizon  $N_c=5$

**Scenario i) Day with High Solar Irradiation.** The disturbances of the virtual distributed solar collector field are shown in (see Fig. 10) where a) is the solar irradiance  $I$  b) is the ambient temperature  $T_{amb}$  c) is the oil inlet temperature  $T_{in}$ . It is observed in (Fig. 11a) that the highest solar irradiation is from 9:06 to 16:18 where the solar irradiation is higher than  $1000 [W/m^2]$ , the lowest solar irradiation is from 8:00 to 9:06 and also from 16:18 to 18:30 in which the solar irradiation remains below  $1000 [W/m^2]$ , the ambient temperature in (Fig. 10b) starts with a value of  $7.35 [^\circ C]$  at 8:00 and ends with a value of  $13.4 [^\circ C]$  at 18:30. For the oil inlet temperature in (Fig. 10c) a constant temperature of  $100 [^\circ C]$  is given throughout the simulation.

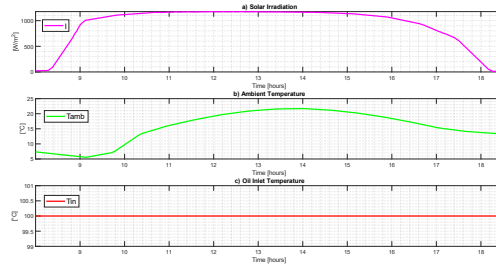


**Fig. 10.** Scenario i): a) Solar irradiation, b) Ambient temperature, c) Oil inlet temperature.

The response of the implemented controllers is shown (see Fig. 11) where (Fig. 11a) corresponds to the response of the controlled variable the oil outlet temperature, where the oil temperature set point (red), the response of the PID control (blue), the response of the MPC (green). (Fig. 11b) and (Fig. 11c) correspond to the responses of the control action oil flow for the PID control and MPC respectively.

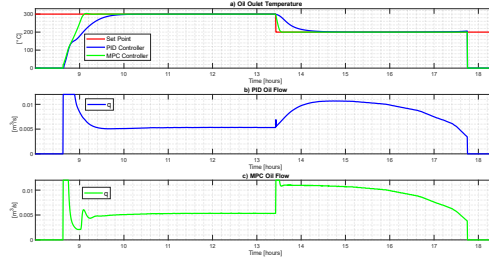


**Fig. 11.** Scenario i): a) Oil outlet temperature, b) PID control oil flow, c) MPC oil flow.

The virtual plant will be in operation (see Fig. 11) from 8:37 to 17:45 since during this period the solar irradiation is higher than  $400 [W/m^2]$ . For the oil outlet temperature, there is a set point of  $300 [^{\circ}C]$  from 8:00 to 13:25, the set point changes to  $200 [^{\circ}C]$  at 13:25 until the end of the simulation.

Looking at the response of the controllers (see Fig. 11a), the PID control with a set point of  $300 [^{\circ}C]$  has an overshoot of 0% and a settling time of 1 hour and 24 minutes, the steady state error is  $6.66 \times 10^{-4}$  which is within the 1% tolerance. On the other hand, the MPC for a set point of  $300 [^{\circ}C]$  has an overshoot of 1.17%, a settling time of 33 minutes, the steady state error is  $1.66 \times 10^{-4}$  which is within the 1% tolerance.

Looking at the response of the control action (see Fig. 11b and Fig. 11c), at the beginning of the operation with a set point of  $300 [^{\circ}C]$  both the PID control and the MPC send 100% of the flow, by the time the set point changes to  $200 [^{\circ}C]$  the PID control sends 40% of the flow while the MPC sends 100% of the flow. It can be said that both the PID control and the MPC have a slow response being the PID control a smoother response compared to the response of the MPC which is a little more aggressive.

**Scenario ii) Day with Medium Solar Irradiation.** The disturbances of the virtual distributed solar collector field are shown in (see Fig. 12) where a) is the solar irradiance  $I$  b) is the ambient temperature  $T_{amb}$  c) is the oil inlet temperature  $T_{in}$ . It is observed in (Fig. 12a) that the highest solar irradiation is from 11:00 to 15:19 where the solar irradiation is higher than  $700 [W/m^2]$ , and it can be seen that the lowest solar irradiation is from 8:00 to 11:00 and also from 15:19 to 18:30 in which the solar irradiation remains below  $700 [W/m^2]$ , the ambient temperature in (Fig. 12b) starts with a value of  $2.59 [^{\circ}C]$  at 8:00 and ends with a value of  $6.69 [^{\circ}C]$  at 18:30. For the oil inlet temperature in (Fig. 12c) a constant temperature of  $100 [^{\circ}C]$  is given throughout the simulation.

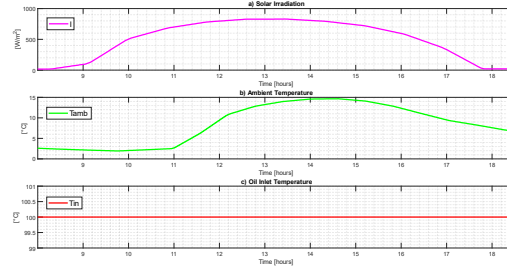


**Fig. 12.** Scenario ii): a) Solar irradiation, b) Ambient temperature, c) Oil inlet temperature.

The response of the implemented controllers is shown (see Fig. 13) where (Fig. 13a) corresponds to the response of the controlled variable the oil outlet temperature, where the oil temperature set point (red), the response of the PID control (blue), the response of the MPC (green). (Fig. 13b) and (Fig. 13c) correspond to the responses of the control action oil flow for the PID control and MPC respectively.

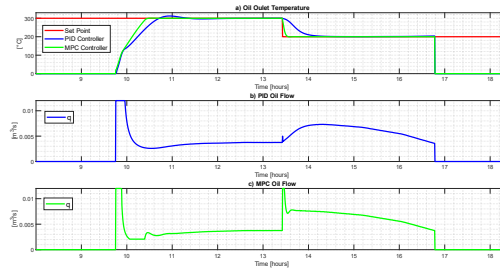


**Fig. 13.** Scenario ii): a) Oil outlet temperature, b) PID control oil flow, c) MPC oil flow.

The virtual plant will be in operation (see Fig. 13) from 9:45 to 16:46 since during this period the solar irradiation is higher than  $400 [W/m^2]$ . For the oil outlet temperature, there is a set point of  $300 [^{\circ}C]$  from 8:00 to 13:25, the set point changes to  $200 [^{\circ}C]$  at 13:25 until the end of the simulation.

Looking at the response of the controllers (see Fig. 13a), the PID control with a set point of  $300 [^{\circ}C]$  has an overshoot of 4% and a settling time of 2 hours and 21 minutes, the steady state error is  $2.33 \times 10^{-3}$  which is within the 1% tolerance. On the other hand, the MPC for a set point of  $300 [^{\circ}C]$  has an overshoot of 0.3%, a settling time of 1 hour, the steady state error is  $1 \times 10^{-3}$  which is within the 1% tolerance.

Looking at the response of the control action (see Fig. 13b and Fig. 13c), at the beginning of the operation with a set point of  $300 [^{\circ}C]$  both the PID control and the MPC send 100% of the flow, by the time the set point changes to  $200 [^{\circ}C]$  the PID control sends 40% of the flow while the MPC sends 100% of the flow. It can be said that both the PID control and the MPC have a slow response being the PID control a smoother response compared to the response of the MPC which is a little more aggressive.

**Scenario iii) Day with Medium Solar Irradiation, the Presence of Clouds, and Variation in the Oil Inlet Temperature.** The disturbances are shown in (see Fig. 14). It is observed in (Fig. 14a) that there is the presence of clouds from 12:00 to 12:37 which causes the solar irradiation to have a value of  $630 [W/m^2]$  during that period. The oil inlet temperature in (Fig. 14c) where a value of  $130 [^{\circ}C]$  is given from 8:00 to 13:43 and then changes to  $90 [^{\circ}C]$  from 13:43 to 18:30. For the ambient temperature in (Fig. 14b) no changes were made because its impact on the oil outlet temperature is insignificant compared to the solar irradiation and inlet oil temperature.

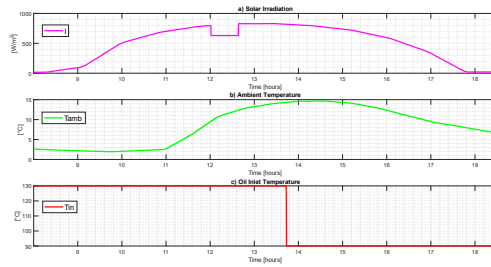


**Fig. 14.** Scenario iii): a) Solar irradiation, b) Ambient temperature, c) Oil inlet temperature.

The response of the implemented controllers is shown (see Fig. 15) where (Fig. 15a) corresponds to the response of the controlled variable the oil outlet temperature, where the oil temperature set point (red), the response of the PID control (blue), the response of the MPC (green). (Fig. 15b) and (Fig. 15c) correspond to the responses of the control action oil flow for the PID control and MPC respectively.

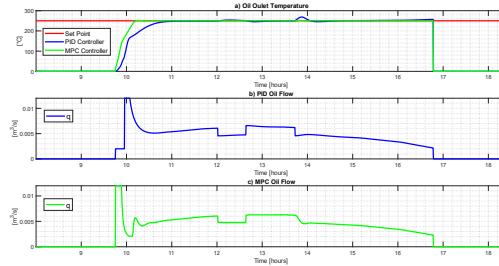


**Fig. 15.** Scenario iii): a) Oil outlet temperature, b) PID control oil flow, c) MPC control oil flow.

The virtual plant will be in operation (see Fig. 15) from 9:45 to 16:46 since during this period the solar irradiation is higher than  $400 [W/m^2]$ . For the oil outlet temperature, a set point of  $250 [^{\circ}C]$  is used for the whole simulation.

Looking at the response of the controllers (see Fig. 15a), the PID control when there is the presence of clouds in the solar irradiation from 12:00 to 12:37 causes an oscillation in the oil outlet temperature with an overshoot of 1.45% and takes 1 hour to resettle for 1% tolerance, when the oil inlet temperature changes to  $90 [^{\circ}C]$  at 13:43 it causes an oscillation in the oil outlet temperature with an overshoot of 7% and takes 43 minutes to resettle for 1% tolerance. For the MPC when there is the presence of clouds in the

solar irradiation from 12:00 to 12:37 it causes a small oscillation in the oil outlet temperature with an overshoot of 0.48%, when the oil inlet temperature changes to 90[°C] at 13:43 it causes an oscillation in the oil outlet temperature with an overshoot of 0.68%, for the 2 disturbances in the MPC the temperature value is still within the tolerance of 1%.

Looking at the response of the control action (see Fig. 15b and Fig. 15c), during the presence of clouds and the variation in the value of oil inlet temperature, the response of the control action for the MPC is smoother compared to the response of the control action for the PID control which is more aggressive causing greater oscillations.

## 6 Conclusions

In this research, a model predictive control MPC strategy and a PID control strategy for a virtual distributed solar collector field are designed and compared.

The implemented virtual environment presents a high realism, it is interactive and immersive. The virtual plant allows the interaction with the components that conform the plant, the visualization of the evolution and state of the variables of interest, as well as allowing the operator to insert disturbances and manipulate the tuning constants of the MPC and PID controllers.

The distributed solar collector field requires efficient controls due to solar irradiation which is its main disturbance and source of energy. It is observed that the MPC has a better performance in the scenarios of high and medium irradiation and in the presence of clouds, presenting an average overshoot of 0.65%, an average settling time of 46 minutes that is less compared to the PID control that has an average overshoot of 3.1% and an average settling time of 1 hour and 22 minutes. Demonstrating that the MPC, due to its shorter settling time, better optimizes the use of solar irradiation available throughout the day. In addition, because it has a low overshoot, it does not exceed the maximum safe temperature of 305 [°C], which the PID control does at certain points of operation. The MPC performs better than the PID control when faced with sudden changes in the oil inlet temperature and the solar irradiation caused by the presence of clouds.

## References

1. Intergovernmental panel on climate change, "Climate Change 2022: Mitigation of Climate Change," 2022.
2. A. Alsharkawi and J. A. Rossiter, "Modelling analysis of a solar thermal power plant," 2017 6th International Conference on Clean Electrical Power (ICCEP), Jun. 2017, doi: 10.1109/iccep.2017.8004766.
3. A. T. Bayas Arévalo, "Diseño de estrategias de control difuso robusto ante incertidumbre paramétrica para plantas de colectores solares," Universidad de Chile, 2016. [Online]. Available: <https://repositorio.uchile.cl/handle/2250/140821>.
4. D. Burgasi, T. Orrala, J. Llanos, D. Ortiz-Villalba, D. Arcos-Aviles, and C. Ponce, "Fuzzy and PID Controllers Performance Analysis for a Combined-Cycle Thermal Power Plant,"

- Recent Advances in Electrical Engineering, Electronics and Energy, pp. 78–93, 2021, doi: 10.1007/978-3-030-72208-1\_7.
5. J. D. Feijoo, D. J. Chanchay, J. Llanos, and D. Ortiz-Villalba, “Advanced Controllers for Level and Temperature Process Applied to Virtual Festo MPS® PA Workstation,” 2021 IEEE International Conference on Automation/XXIV Congress of the Chilean Association of Automatic Control (ICA-ACCA), Mar. 2021, doi: 10.1109/icaacca51523.2021.9465269.
  6. J. Llanos-Proano, M. Pilatasig, D. Curay, and A. Vaca, “Design and implementation of a model predictive control for a pressure control plant,” 2016 IEEE International Conference on Automatica (ICA-ACCA), Oct. 2016, doi: 10.1109/ica-acca.2016.7778490.
  7. T. Orrala, D. Burgasi, J. Llanos, and D. Ortiz-Villalba, “Model Predictive Control Strategy for a Combined-Cycle Power-Plant Boiler,” 2021 IEEE International Conference on Automation/XXIV Congress of the Chilean Association of Automatic Control (ICA-ACCA), Mar. 2021, doi: 10.1109/icaacca51523.2021.9465302.
  8. L. Aimacaña, O. Gahui, J. Llanos, and D. Ortiz, “Advanced Control Algorithms for a Horizontal Three-Phase Separator in a Hardware in the Loop Simulation Environment.,” CIT, 2022.
  9. F. Camacho, M. Berenguel, and F. R. Rubio, “Advanced Control of Solar Plants,” *Advances in Industrial Control*, 1997, doi: 10.1007/978-1-4471-0981-5.
  10. L. J. Yebra, M. Berenguel, J. Bonilla, L. Roca, S. Dormido, and E. Zarza, “Object-oriented modelling and simulation of ACUREX solar thermal power plant,” *Mathematical and Computer Modelling of Dynamical Systems*, vol. 16, no. 3, pp. 211–224, Oct. 2010, doi: 10.1080/13873954.2010.507420.
  11. E. F. Camacho, F. R. Rubio, M. Berenguel, and L. Valenzuela, “A survey on control schemes for distributed solar collector fields. Part I: Modeling and basic control approaches,” *Sol. Energy*, vol. 81, no. 10, pp. 1240–1251, Oct. 2007, doi: 10.1016/j.solener.2007.01.002.
  12. Ricardo Carmona Contreras, “Análisis, modelado y control de un campo de colectores solares distribuidos con un sistema de seguimiento de un eje.,” Universidad de Sevilla, España, 1985.
  13. V. H. Andaluz, D. Castillo-Carrión, R. J. Miranda, and J. C. Alulema, “Virtual Reality Applied to Industrial Processes,” *Augmented Reality, Virtual Reality, and Computer Graphics*, pp. 59–74, 2017, doi: 10.1007/978-3-319-60922-5\_5.
  14. J. S. Ortiz, G. Palacios-Navarro, V. H. Andaluz, and B. S. Guevara, “Virtual Reality-Based Framework to Simulate Control Algorithms for Robotic Assistance and Rehabilitation Tasks through a Standing Wheelchair,” *Sensors*, vol. 21, no. 15, p. 5083, Jul. 2021, doi: 10.3390/s21155083.
  15. “Self-tuning control of a solar power plant with a distributed collector field,” *IEEE Control Systems*, vol. 12, no. 2, pp. 72–78, Apr. 1992, doi: 10.1109/37.126858.
  16. E. Pruna, E. R. Sasig, and S. Mullo, “PI and PID controller tuning tool based on the lambda method,” 2017 CHILEAN Conference on Electrical, Electronics Engineering, Information and Communication Technologies (CHILECON), Oct. 2017, doi: 10.1109/chilecon.2017.8229616.
  17. B. Kouvaritakis and M. Cannon, “Model Predictive Control,” *Advanced Textbooks in Control and Signal Processing*, 2016, doi: 10.1007/978-3-319-24853-0.
  18. “JRC Photovoltaic Geographical Information System (PVGIS) - European Commission.” [https://re.jrc.ec.europa.eu/pvg\\_tools/es/](https://re.jrc.ec.europa.eu/pvg_tools/es/).